

Recoil-separated gamma-ray spectroscopy of ^{47}Ti , ^{47}V , ^{47}Cr , ^{48}V , and ^{48}Cr

J. A. Cameron

*Department of Physics and Astronomy, McMaster University, Hamilton, Ontario, Canada L8S 4K1*M. A. Bentley,* A. M. Bruce,† R. A. Cunningham, W. Gelletly,‡ H. G. Price, J. Simpson, and D. D. Warner
Science and Engineering Research Council Daresbury Laboratory, Warrington, WA4 4AD, United Kingdom

A. N. James

*Oliver Lodge Laboratory, Department of Physics, Liverpool University,
Liverpool, L69 3BX, United Kingdom*

(Received 5 August 1993)

High-spin states in the nuclei ^{47}Ti , ^{47}V , ^{47}Cr , ^{48}V , and ^{48}Cr have been observed using the reaction $^{40}\text{Ca}+^{10}\text{B}$ at $E(^{40}\text{Ca})=150$ MeV. The prompt γ rays were detected in an array of 19 escape-suppressed Ge detectors in coincidence with the recoiling nuclei which were identified in A and Z with a recoil separator. Rotational structures were observed in all these nuclei, apart from ^{47}Ti , up to spins near the maximum for the $(f_{7/2})^{z+n}$ configuration. A rapid increase in the Coulomb displacement energy for mirror states in ^{47}V and ^{47}Cr occurs at $J^\pi = 25/2^-$. A backbend occurs in ^{48}Cr at $J^\pi = 10^+$.

PACS number(s): 23.20.Lv, 27.40.+z

I. INTRODUCTION

The spectroscopy of the nuclei from Ca to Ni is for the most part well described by the shell model. The low-lying structure has been found to be fairly well represented by $(f_{7/2})^{z+n}$ calculations such as those of Kutschera, Brown, and Ogawa [1] with intruder states from the pf shell above and sd shell below. Within the context of the isolated $f_{7/2}$ shell, one expects cross-conjugate symmetry in addition to the more generally applicable mirror symmetry. The $f_{7/2}$ shell is the only nontrivial proving ground for the former symmetry, and beyond it the valley of stability deviates too far from $N = Z$ to make detailed spectroscopy of mirror pairs currently practicable.

On the other hand, it has been known for some time that nuclei near the middle of the $f_{7/2}$ shell (i.e., $^{48}\text{Cr} \pm 1$ nucleon) show some collectivity near the ground state. The $B(E2)$ for the $2^+ \rightarrow 0^+$ transition in ^{48}Cr is $220 e^2\text{fm}^4$ (21 W.u.) [2], implying a deformation parameter of $\beta = 0.35$, or a ratio of major to minor axes of 1.6:1. The yrast levels of ^{48}Cr and its better-studied neighbors, ^{49}Cr and ^{47}V , follow approximately a $J(J+1)$ energy scale up to a spin of about 8 [3,4]. It is possible within the $(f_{7/2})^{z+n}$ shell model to reproduce some degree of collectivity at moderate spins, but the large number of components in the shell-model wave functions required

to produce such properties in the yrast states is greatly reduced near the band termination at $J_{\text{max}} = [z(8-z) + n(8-n)]/2$. Recently, much interest has been focused on the production and stability of nuclear states of very large deformation. Known to exist in much heavier nuclei, such states are also predicted to occur in a few light nuclei. In particular, ^{48}Cr is expected to have a high-energy band of states with a 3:1 axis ratio [5].

This region of nuclei thus offers the unique opportunity to study a combination of phenomena not normally associated with each other: mirror and cross-conjugate symmetries and collective features such as band crossing and extreme deformation. In order to investigate these issues and to shed light on the detailed relation between the collective and individual particle motions, experiments are needed which can probe light nuclei to high energies and spins, that is, near $J = 16$ and $E = 10$ MeV. A series of experiments was undertaken in this region [6,7] to investigate these phenomena.

Spectroscopy of light nuclei at high spin and energy is encumbered by a number of difficulties, the most obvious of which arise from the low mass, radius, and charge. The first leads to high recoil velocities in compound nucleus reactions and the second to high γ -ray transition energies. Therefore, the problem of Doppler shifts and the consequent degradation in γ -ray energy resolution is severe. The low Z of the systems involved in reaction studies with light nuclei allows a proliferation of reaction channels with proton and alpha emission competing strongly with neutron decay of the compound nucleus and it is not uncommon for there to be five or six strongly competing exit channels. It becomes important to identify these in analyzing γ -ray spectra, either by observing the light decay fragments or the γ -emitting recoil ions.

In the first f -shell experiment carried out with the

*Present address: School of Sciences, Staffordshire University, College Road, Stoke-on-Trent, ST4 2DE, UK.

†Present address: Department of Mathematical Studies, University of Brighton, Brighton, BN2 4GJ, UK.

‡Present address: Physics Department, University of Surrey, Guildford, Surrey, GU2 5XH, UK.

Daresbury 0° recoil mass separator [8] and escape-suppressed Ge detector array [9], spectra of the mirror pair ^{49}Cr - ^{49}Mn , as well as ^{49}V and ^{46}Ti were cleanly separated in both A and Z , and level structures were derived from recoil- γ and recoil- γ - γ spectra [6,7]. In the present experiment, the study was extended to the $A = 47$ and 48 isobars Ti, V, and Cr. The mirror nuclei ^{47}V - ^{47}Cr

were observed up to the $J_{\text{max}} = 31/2$ band termination and the remainder to levels at little below J_{max} . In the mirror pair, an alignment-related change in the Coulomb energy difference was found, as in the cross-conjugate $A = 49$ case, whereas only a small change was seen in the moment of inertia. A backbend was found in ^{48}Cr near $J = 10$.

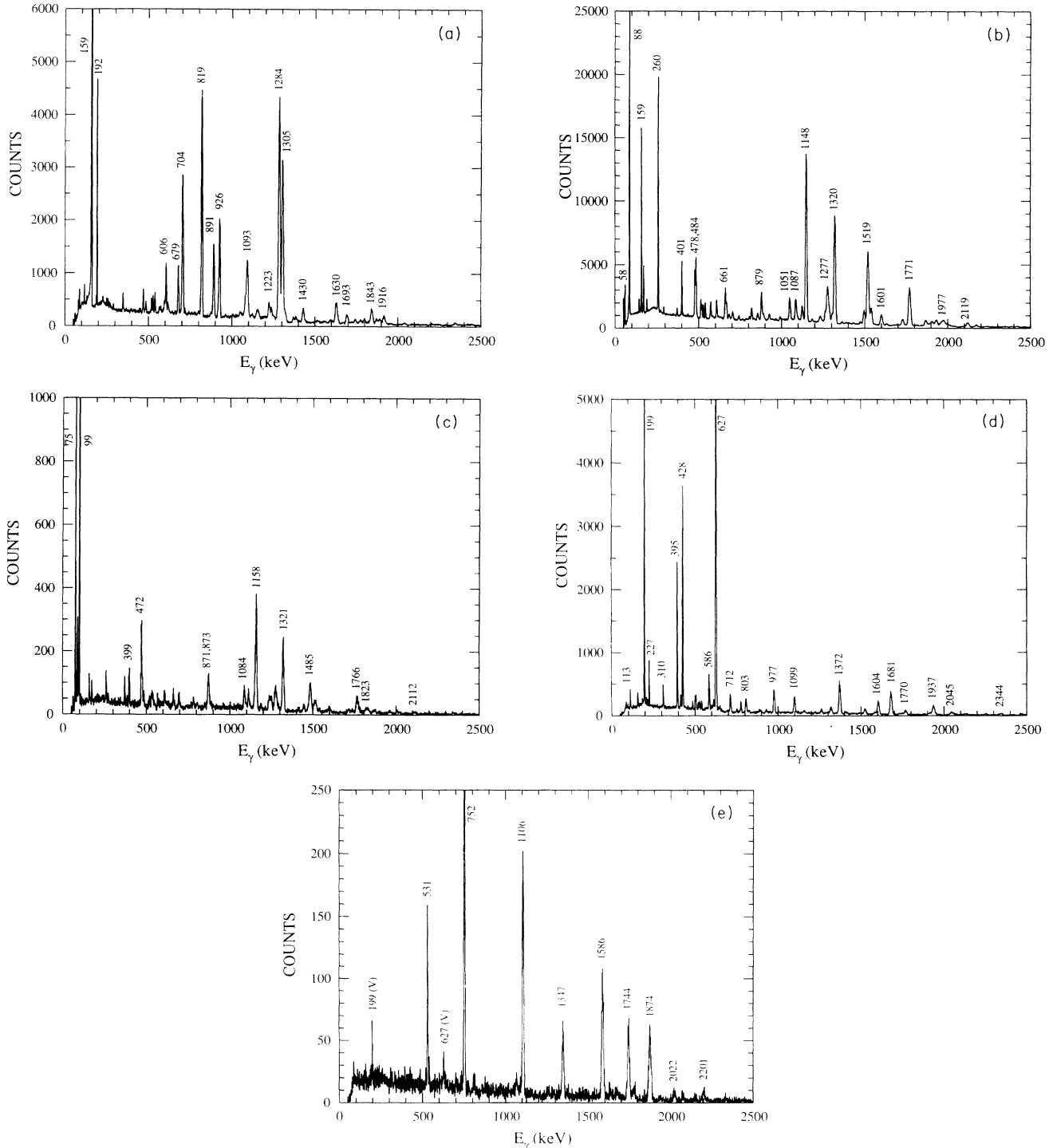


FIG. 1. Gamma-ray spectra for (a) ^{47}Ti , (b) ^{47}V , (c) ^{47}Cr , (d) ^{48}V , and (e) ^{48}Cr , recorded in recoil- γ coincidence, with gating on the appropriate position (A), E and ΔE information from the recoil-separator detectors.

II. EXPERIMENT

The reaction $^{10}\text{B}(^{40}\text{Ca}, xpn)$ at $E_{\text{Ca}} = 150$ MeV was used to produce the $A = 47$ isobars Ti, V, and Cr in the three-nucleon exit channels, and ^{48}V and ^{48}Cr in the $2p$ and pn exit channels. Target impurities of ^{11}B and ^{12}C

led to other residues, notably ^{48}Ti and ^{50}Cr . The recoil nuclei were separated, as in Refs. [6,7], using the Daresbury 0° recoil separator, set to accept $A = 47$ and 48 at the optimum ionic charge of 17^+ . Single γ and coincident γ - γ events in coincidence with A - and Z -selected recoil ions were recorded.

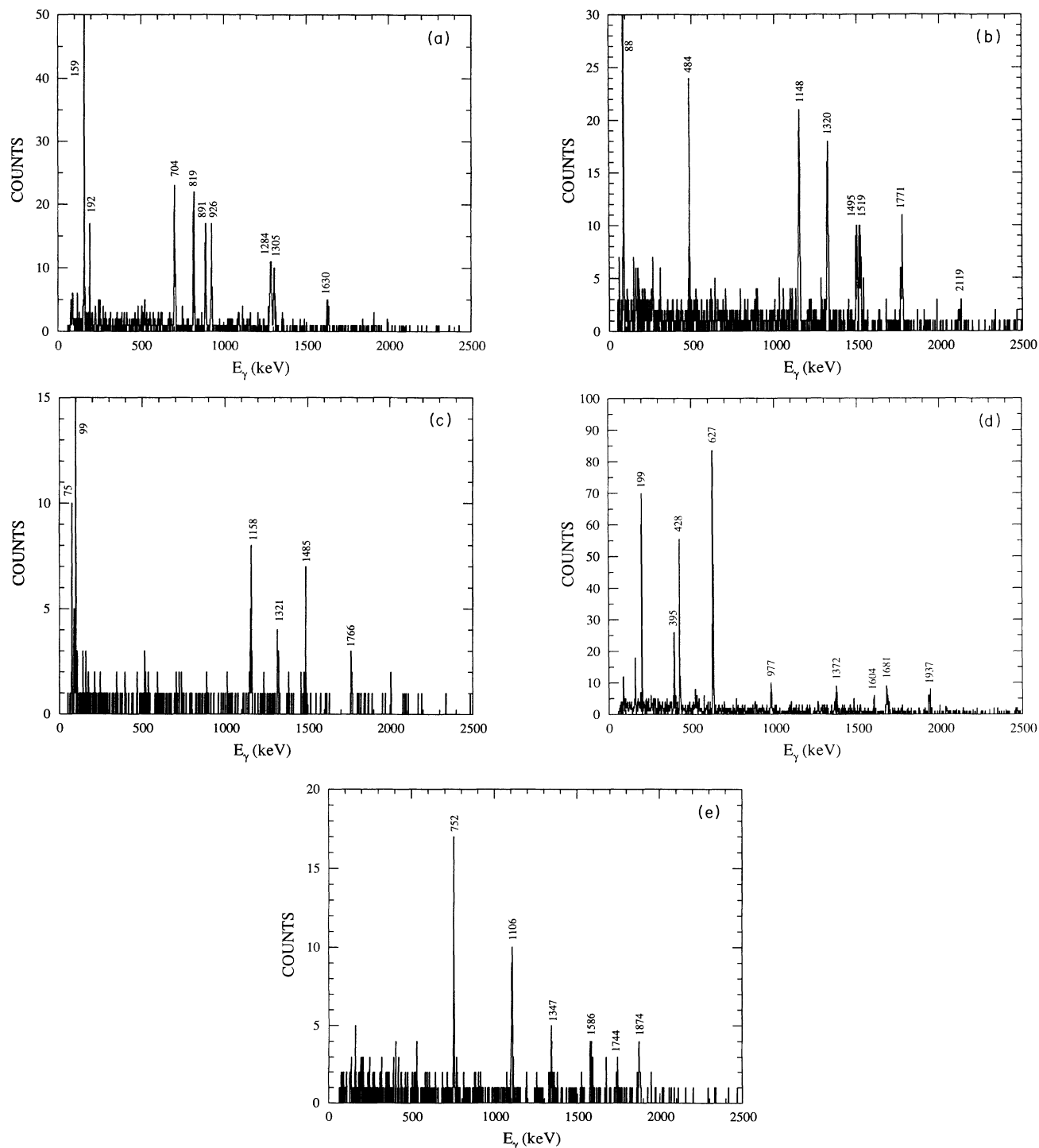


FIG. 2. Recoil γ - γ coincidence spectra for (a) ^{47}Ti (gate: 891 keV), (b) ^{47}V (gate: 486 keV), (c) ^{47}Cr (sum of gates: 1158, 1321, 1485, 1766 keV), (d) ^{48}V (sum of gates: 395, 1371, 1681, 1937 keV), (e) ^{48}Cr (sum of gates: 752, 1106, 1347, 1586, 1744, 1874 keV).

In all, 10^8 events were recorded, with 3×10^6 involving two or more gamma rays. With the mass-47 and -48 recoil gates, respectively, 2×10^6 and 2×10^5 single gamma events and 1.2×10^5 and 1.5×10^4 γ - γ coincidences were detected. The relative yields of events in the major reaction channels were $3p+^{47}\text{Ti}$ (36), $2pn+^{47}\text{V}$ (100), $p2n+^{47}\text{Cr}$ (3.2), $2p+^{48}\text{V}$ (12), $pn+^{48}\text{Cr}$ (1.3). Although the recoil- γ - γ matrices contain relatively few events, they are free from contamination and could be analyzed in the normal way, even for the weaker reaction products ^{47}Cr and ^{48}Cr . In general, the γ - γ data showed too much cross contamination to be useful in the analysis.

In the focal plane of the recoil separator, the dominant mass-47 and mass-48 peaks (charge state 17^+) were cleanly separated in the position detector (FWHM $\simeq 0.3$ mass units). In addition, recoils with mass to charge state ratio $A/Q = \frac{50}{18}$ appeared in the $\frac{47}{17}$ peak and $A/Q = \frac{44}{16}$ under the $\frac{48}{17}$ peak. These A/Q ambiguities could be partly removed by further selection using the total-energy E signal from the ionisation detector. The lighter recoils deposit a lower total energy, as demonstrated in Fig. 1 of Ref. [7] which shows a displacement of ^{46}Ti recoils from mass-49 ions in a reaction similar to the present one. As Refs. [6,7] demonstrated, excellent Z separation is achieved in the ionization $E\Delta E$ detector because of the high recoil velocity ($v/c = 0.07$). The FWHM of the ΔE projection, in the present experiment as in the $A = 49$ study, was $\Delta Z \simeq 0.5$.

The calibration in energy and relative efficiency of each of the 19 Ge detectors was made using a ^{152}Eu source. Correction for the Doppler shifts was made in playback of the data. Both the energy calibration and Doppler corrections were confirmed using prominent reaction lines. The overall spectral resolution is dominated by the Doppler broadening due to the detector apertures, particularly at 101° and 117° . For the two- and three-nucleon channels of primary interest, the measured linewidth (FWHM) was 0.8% above 1 MeV. The resulting precision of the spectroscopy is, for strong lines, about 0.2%, and the resulting level energies, usually supported by more than one transition, have a precision of about 1 keV.

The 19 Ge detectors were arranged in four rings, at 40° , 101° , 117° , and 143° to the beam direction. Angular anisotropies of γ rays were obtained by summing the 40° and 143° intensities and comparing with the 101° intensity. Figure 3 of Ref. [7] indicates how the anisotropy

$$A = \frac{W(40) + W(143)}{2W(101)}$$

depends on $J_i - J_f$ and δ . The most important ambiguity occurs for $J \rightarrow J - 2$ and $J \rightarrow J$ transitions. The intensity at 117° does not help to resolve such ambiguities.

III. RESULTS

The pure recoil-gated singles γ -ray spectra for ^{47}Ti , ^{47}V , ^{47}Cr , ^{48}V and ^{48}Cr are shown in Fig. 1. Figure 2 shows examples of the recoil-gated γ - γ spectra for each

of the nuclei. Gating details are given in the captions. Tables I-V contain the energies, intensities, and angular anisotropies measured in each case, ordered according to the deduced energy level schemes. The level schemes

TABLE I. States and transitions in ^{47}Ti .

E_i (keV)	E_f (keV)	E_γ (keV)	Int. % ^a	A^b	J_i^π	J_f^π
159	0	159	~ 100	0.93(1)	$\frac{7}{2}^-$	$\frac{5}{2}^-$
1252	159	1093	20	1.01(3)	$\frac{9}{2}^-$	$\frac{7}{2}^-$
	0	1252	1			
1444	159	1284	80	1.37(2)	$\frac{11}{2}^-$	$\frac{7}{2}^-$
	1252	192	5	0.84(3)		$\frac{9}{2}^-$
2406	159	2247	1		$\frac{9}{2}^-$	$\frac{7}{2}^-$
	1252	1154	3			$\frac{9}{2}^-$
	1444	962	0.3			$\frac{11}{2}^-$
2682	1252	1430	7	0.94(6)	$\frac{11}{2}^{(-)}$	$\frac{9}{2}^-$
	1444	1238	3	1.8(3)		$\frac{11}{2}^-$
	2406	276	0.1			$\frac{9}{2}^-$
2749	1444	1305	60	1.40(2)	$\frac{15}{2}^-$	$\frac{11}{2}^-$
3288	1252	2037	1		$\frac{13}{2}^-$	$\frac{9}{2}^-$
	1444	1843	9	0.89(5)		$\frac{11}{2}^-$
	2682	606	4	0.66(3)		$\frac{11}{2}^-$
3568	2749	819	40	0.87(2)	$\frac{17}{2}^-$	$\frac{15}{2}^-$
3727	1252	2475	0.3		$\frac{13}{2}^-$	$\frac{9}{2}^-$
	2406	1321	4	1.5(2)		$\frac{9}{2}^-$
3994	1444	2550	1		$\frac{15}{2}^-$	$\frac{11}{2}^-$
	3288	706	8	0.7(2)		$\frac{13}{2}^-$
	3727	267	0.1			$\frac{13}{2}^-$
4494	2749	1745	2	1.7(4)	$\frac{19}{2}^-$	$\frac{15}{2}^-$
	3568	926	20	0.89(2)		$\frac{17}{2}^-$
4673	2749	1924	1		$\frac{17}{2}^-$	$\frac{15}{2}^-$
	3288	1385	2	2.0(4)		$\frac{13}{2}^-$
	3994	679	6	0.78(3)		$\frac{15}{2}^-$
5198	3568	1630	14	1.26(6)	$\frac{21}{2}^-$	$\frac{17}{2}^-$
	4494	704	12	0.9(2)		$\frac{19}{2}^-$
6089	4494	1595	2	1.0(1)	$\frac{23}{2}^-$	$\frac{19}{2}^-$
	5198	891	14	0.90(2)		$\frac{21}{2}^-$
6366	3568	2798	1		$\frac{21}{2}^-$	$\frac{17}{2}^-$
	4494	1873	3	1.6(3)		$\frac{19}{2}^-$
	4673	1693	5	1.4(2)		$\frac{17}{2}^-$
8005	6089	1916	6	1.3 (1)	$\frac{27}{2}^-$	$\frac{23}{2}^-$

^aNormalized to 100 for the sum of decays to the ground state.

^bSee text, Sec. II. Uncertainties 1σ .

themselves are presented in Figs. 3-7. The placement of levels was made using intensities, energy sums (in cases of cascade-crossover loops), and coincidence relationships. Spin-parity combinations were deduced from the observed recoil- γ angular anisotropies.

A. The level scheme of ^{47}Ti

The level scheme of ^{47}Ti , produced through the $3p$ exit channel, is shown in Fig. 3. All states, apart from the $\frac{13}{2}$ state at 3727 keV, had been observed previously. However, a number of previously unobserved γ rays were found and angular distributions were measured, allowing a more complete assignment of spins and parities to known levels (Table I and Fig. 3). In the yrast band, the 1745-, 1598-, and 1630-keV crossover transitions establish the negative parity of the 4494-, 5198-, and 6089-keV levels. The top 1916-keV transition seems likely to

be stretched $E2$.

The sideband based on the level at 2682 keV was known previously, but its parity had not been determined. The spin- $\frac{13}{2}$, $-\frac{15}{2}$, and $-\frac{21}{2}$ levels have weak quadrupole decays, presumed to be $E2$, to the yrast $\frac{9}{2}^-$, $\frac{11}{2}^-$, and $\frac{17}{2}^-$ states, respectively, and the $\frac{13}{2}$ and $\frac{21}{2}$ levels are similarly connected with the $\frac{17}{2}$ level at 4673 keV. This establishes the parity of all the levels of the band to be negative, with the possible exception of the $\frac{11}{2}$ state. The separate side levels, $\frac{9}{2}$ and $\frac{13}{2}$ at 2406 and 3727 keV, respectively, are connected by a quadrupole transition and the latter decays weakly to the yrast $\frac{9}{2}^-$ state, so both have negative parity.

B. The level scheme of ^{47}V

This was the most abundant product in the reaction, accounting for almost half the observed events. Accord-

TABLE II. States and transitions in ^{47}V .

E_i (keV)	E_f (keV)	E_γ (keV)	Int. % ^a	A^b	J_i^π	J_f^π	E_i (keV)	E_f (keV)	E_γ (keV)	Int. % ^a	A^b	J_i^π	J_f^π
88	0	88	~60	1.44(2)	$\frac{5}{2}^-$	$\frac{3}{2}^-$	2558	1272	1286	8	1.4(2)	$\frac{13}{2}^-$	$\frac{9}{2}^-$
													$\frac{11}{2}^-$
146	0	146	0.3	1.4(2)	$\frac{7}{2}^-$	$\frac{3}{2}^-$							
	88	58	~60			$\frac{5}{2}^-$	2614	1294	1320	50	1.21(1)	$\frac{15}{2}^-$	$\frac{11}{2}^-$
										~1			$\frac{13}{2}^-$
260	0	260	7	1.0(1)	$\frac{3}{2}^+$	$\frac{3}{2}^-$							
	88	172	1			$\frac{5}{2}^-$	3272	1294	1978 ^c	0.6		$\frac{13}{2}^+$	$\frac{11}{2}^-$
													$\frac{9}{2}^+$
661	0	661	4	0.98(4)	$\frac{5}{2}^+$	$\frac{3}{2}^-$							
	88	573	2	1.48(9)		$\frac{5}{2}^-$					1.39(4)		$\frac{11}{2}^+$
	146	514	2			$\frac{7}{2}^-$	3955	2416	1539	11	1.52(5)	$\frac{15}{2}^+$	$\frac{11}{2}^+$
	260	401	3	0.85(2)		$\frac{3}{2}^+$							$\frac{13}{2}^+$
1139	88	1051	7	0.95(3)	$\frac{7}{2}^+$	$\frac{5}{2}^-$	4133	2614	1519	40	1.39(2)	$\frac{19}{2}^-$	$\frac{15}{2}^-$
	146	992	1	1.9(4)		$\frac{7}{2}^-$							
	260	879	6	1.09(3)		$\frac{3}{2}^+$	5001	2614	2387	1.5		$\frac{17}{2}^+$	$\frac{15}{2}^-$
	661	478	4	0.82(2)		$\frac{5}{2}^+$					1.40(9)		$\frac{13}{2}^+$
1272	88	1184	1		$\frac{9}{2}^-$	$\frac{5}{2}^-$	5904	4133	1771	30	1.39(2)	$\frac{23}{2}^-$	$\frac{19}{2}^-$
	146	1126	5	1.15(4)		$\frac{7}{2}^-$							
							5886	3955	1931	6	1.33(6)	$\frac{19}{2}^+$	$\frac{15}{2}^+$
1294	146	1149 ^c	60	1.31(1)	$\frac{11}{2}^-$	$\frac{7}{2}^-$	6870	5001	1869	6	1.32(6)	$\frac{21}{2}^+$	$\frac{17}{2}^+$
													$\frac{23}{2}^-$
1748	146	1601	8	0.92(3)	$\frac{9}{2}^+$	$\frac{7}{2}^-$							
	661	1087	8	1.08(4)		$\frac{5}{2}^+$	7399	5904	1495	9	0.82(2)	$\frac{25}{2}^-$	$\frac{23}{2}^-$
	1139	609	2			$\frac{7}{2}^+$							
							7883	5904	1978 ^c	5	1.8(3)	$\frac{27}{2}^-$	$\frac{23}{2}^-$
2416	1139	1277	16	1.3(1)	$\frac{11}{2}^+$	$\frac{7}{2}^+$							
	1272	1145 ^c	0.6			$\frac{9}{2}^-$					1.0(1)		$\frac{25}{2}^-$
	1748	668	2	0.70(4)		$\frac{9}{2}^+$	10002	7883	2119	5	1.39(8)	$\frac{31}{2}^-$	$\frac{27}{2}^-$

^aNormalized to 100 for total feeding to 0-, 88-, 146-keV levels.

^bSee text, Sec. II. Uncertainties are 1σ .

^cDoublet, intensities from coincidence spectra.

ingly, considerable extension of the level scheme (Table II and Fig. 4) has been possible. The yrast band is extended from the previously established $\frac{23}{2}^-$ level up to $\frac{31}{2}^-$. The positive-parity band built on the known $\frac{3}{2}^+$

260-keV state could be seen from its previous limit at $\frac{9}{2}^+$ up to $\frac{21}{2}^+$. The two band-connecting $E1$ transitions, at 1145 and 1978 keV, are weak members of doublets so their intensities are uncertain.

TABLE III. States and transitions in ^{47}Cr .

E_i (keV)	E_f (keV)	E_γ (keV)	Int. % ^a	A^b	J_i^π	J_f^π
99	0	99	~70	1.06(4)	$\frac{5}{2}^-$	$\frac{3}{2}^-$
174	0	174	1		$\frac{7}{2}^-$	$\frac{3}{2}^-$
	99	75	~70			$\frac{5}{2}^-$
472	0	472	12	1.3(2)	$\frac{3}{2}^+$	$\frac{3}{2}^-$
	99	372	2	1.2(3)		$\frac{5}{2}^-$
871	0	871	10	0.9(1)	$\frac{5}{2}^+$	$\frac{3}{2}^-$
	99	770	1			$\frac{5}{2}^+$
	472	399	3	0.8(1)		$\frac{3}{2}^+$
1332	174	1158	70	1.33(7)	$\frac{11}{2}^-$	$\frac{7}{2}^-$
1345	99	1248	3		$\frac{7}{2}^+$	$\frac{5}{2}^-$
	472	873	9			$\frac{3}{2}^+$
	871	474	12	1.3(2)		$\frac{5}{2}^+$
1955	174	1781	5		$\frac{9}{2}^+$	$\frac{7}{2}^-$
	871	1088	12	1.2(2)		$\frac{5}{2}^+$
	1345	610	1			$\frac{7}{2}^+$
2618	1332	1286	6		$\frac{11}{2}^+$	$\frac{11}{2}^-$
	1345	1273	20	1.6(2)		$\frac{7}{2}^+$
	1955	662	1			$\frac{9}{2}^+$
2653	1332	1321	60	1.33(9)	$\frac{15}{2}^-$	$\frac{11}{2}^-$
3470	1955	1514	20	1.6(3)	$\frac{13}{2}^+$	$\frac{9}{2}^+$
	2618	852	1			$\frac{11}{2}^+$
3765	2653	1112	9	0.6(1)	$\frac{17}{2}^-$	$\frac{15}{2}^-$
4138	2653	1485	40	1.3(1)	$\frac{19}{2}^-$	$\frac{15}{2}^-$
	3765	372	2			$\frac{17}{2}^-$
4215	2618	1597	4		$\frac{15}{2}^+$	$\frac{11}{2}^+$
	3470	744	1			$\frac{13}{2}^+$
5374	4138	1236	10	0.5(1)	$\frac{21}{2}^-$	$\frac{19}{2}^-$
5904	4138	1766	30	1.2(2)	$\frac{23}{2}^-$	$\frac{19}{2}^-$
	5374	530	4			$\frac{21}{2}^-$
7727	5904	1823	11	2.3(9)	$\frac{27}{2}^-$	$\frac{23}{2}^-$
9839	7727	2112	4		$\frac{31}{2}^-$	$\frac{27}{2}^-$

^aNormalized to 100 for sum of decays to 0-, 99-, and 174-keV levels.

^bSee text, Sec. II. Uncertainties are 1σ .

C. The level scheme of ^{47}Cr

This nucleus populated at about $\frac{1}{30}$ th of the intensity of ^{47}V was still strong enough to be seen, and to allow angular distribution measurements, up to the $\frac{31}{2}^-$ state (Table III, Fig. 5). Previously, levels up to $\frac{15}{2}^-$ were known, although all spins were uncertain.

D. The level scheme of ^{48}V

The self-conjugate odd-odd nuclide ^{48}V has been studied previously by many groups [2,10]. Here it was strongly populated, and the yrast band, known previously up to 13^+ [10], has been confirmed and extended by two further transitions to 15^+ . The band based on the 4^- state at 1099 keV was established up to 4390 keV (9^-). The second negative-parity band based on the 1^- state at 518 keV was established to the 2062-keV (5^-) level. A 717-keV decay to the 5^- state was seen weakly but the expected 1222-keV transition, if present, was obscured by the more intense 1223-keV line from the more intense 4^- band. An imputed 6^- level at 2779 keV is therefore uncertain and is not included in Fig. 6. Many of the weak transitions connecting the bands are reported here for the first time.

E. The level scheme of ^{48}Cr

States in ^{48}Cr have been proposed previously [2] up to spin 9 or 10 at 7070 keV. This work established the 7062-keV level as 10^+ (Table V and Fig. 7) and extends the level scheme up to 10609 keV (14^+). The 8^+ is established at 5318 rather than 5189 keV as reported previously. This change results from a reversal of the 1744- and 1874-keV transitions based on their relative intensities. Further intensity below the new location of the 8^+ is provided by the 806–1068-keV cascade through a level at 4512 keV, likely of spin 7^+ , since no evidence for decays to the negative-parity levels or to the 4^+ state was found.

IV. DISCUSSION

A. ^{48}Cr

The nucleus ^{48}Cr , at the center of the $f_{7/2}$ shell, has a rotational level structure at low spin. With the reordering of the transitions near 8^+ and the extension to higher spins, a clear backbend becomes apparent, signaling a band crossing. This is most clearly seen in Fig. 8, a plot of the rotational energy $\hbar\omega = [E(J) - E(J-2)]/2$

TABLE IV. States and transitions in ^{48}V .

E_i (keV)	E_f (keV)	E_γ (keV)	Int. % ^a	A^b	J_i^π	J_f^π	E_i (keV)	E_f (keV)	E_γ (keV)	Int. % ^a	A^b	J_i^π	J_f^π
308	0	308	0.2		2^+	4^+	2062	613	1449	1		5^-	4^+
								1055	1007	1			3^-
421	308	113	1		1^+	2^+		1557	505	2			4^-
428	0	428	30	0.89(2)	5^+	4^+	2232	627	1604	20	1.4(1)	8^+	6^+
								1255	977	15	0.69(4)		7^+
518	308	210	0.6		1^-	2^+							
	421	97	0.2			1^+	2397	428	1969	1		6^-	5^+
								627	1770	6	1.2(2)		6^+
613	0	613	2		4^+	4^+		1685	712	6	0.72(6)		5^-
	428	186	0.3			5^+							
							2627	1255	1372	40	1.30(6)	9^+	7^+
627	0	627 ^c	55		6^+	4^+		2232	395	20	0.89(3)		8^+
	428	199	30	0.82(2)		5^+							
							3173	627	2546	2		7^-	6^+
745	518	227	3	0.89(7)	2^-	1^-		2397	776	5	0.71(8)		6^-
1055	518	537	<0.2		3^-	1^-	3976	2232	1744	2		8^-	8^+
	613	441	0.2			4^+		2397	1588	3	1.7(4)		6^-
	745	310	2			4^+		2627	1349	0.7			9^+
								3173	803	6	1.06(9)		7^-
1099	0	1099	13	1.3(1)	4^-	4^+							
	613	486	1			4^+	4308	2627	1681	40	1.52(8)	11^+	9^+
1255	428	825	1		7^+	5^+	4390	3137	1223	0.6		9^-	7^-
	627	628 ^c	40			6^+		3976	414	2	0.9(1)		8^-
1557	745	812	2		4^-	2^-	6245	4308	1937	20	1.4(1)	13^+	11^+
	1055	502	2			3^-							
	1099	458	0.4			4^-	8290	6245	2045	7	1.4(1)	15^+	13^+
1685	1099	586	9	0.71(4)	5^-	4^-	8539	6245	2344	3	0.8(2)	14^+	13^+

^aNormalized to 100 for decays to the ground state.

^bSee text, Sec. II. Uncertainties are 1σ .

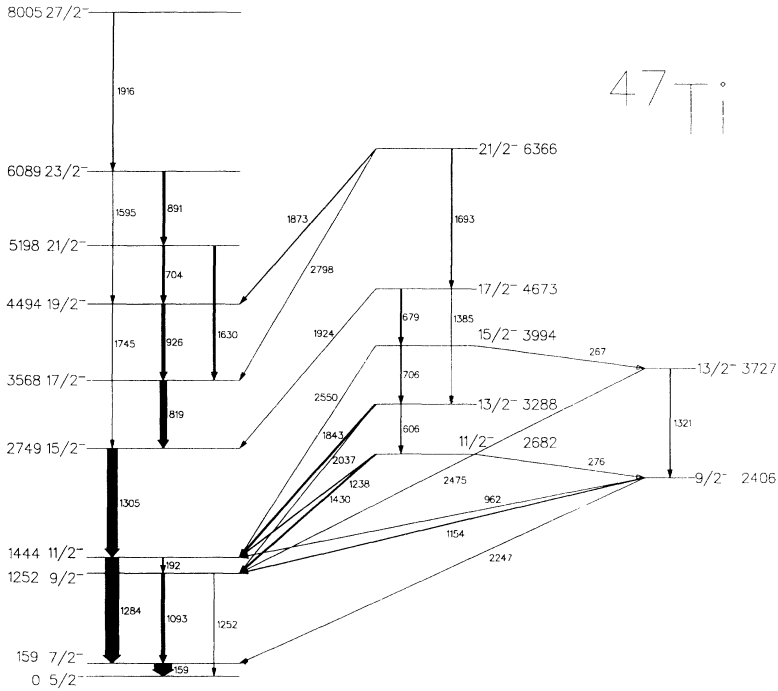
^cDoublet, intensities from coincidence spectra.

against spin $J - 1$. Moreover, the increase in spin, measured by the vertical separation of the branches, amounts to $\sim 6\hbar$ and represents the alignment occurring as a result of the band crossing. This result represents the first observation of the alignment in an $N = Z$ nucleus, and raises some important questions concerning the role of neutron-proton pairing in the collective structure of such nuclei.

The need for inclusion of $T = 0$ pairing in the ground-state correlations was investigated some time ago for lighter nuclei via generalized Hartree-Fock-Bogoliubov calculations [11] which incorporate both $T = 0$ and 1 pairing. The results indicate that the $T = 0$ pairing mode invariably dominates in $N = Z$ nuclei, with $T = 1$ competition increasing with neutron excess. Thus, for $N = Z + 2$ there is competition between the two modes, and for $N \geq Z + 4$ only $T = 1$, $T_z = \pm 1$ need be considered. The competition between the two modes can be understood qualitatively in terms of the stronger binding

of the $T = 0$ mode being counterbalanced by the increasing number of $T_z = \pm 1$ pairs which are possible with increasing neutron excess.

The alignment phenomenon, which occurs as the collective rotational frequency increases, involves the breaking of a pair of nucleons and the subsequent realignment of their angular momenta parallel to the rotation axis. The full cranked shell-model (CSM) calculations that account for such features have not, as yet, included the possibility of neutron-proton pairing. However, the results of a recent theoretical study [12] suggest that yrast band crossings for $N = Z$ may indeed be significantly affected by the residual neutron-proton correlations. One of the predictions of that study is that the two-quasiparticle band crossing which gives rise to the alignment can be described by a linear superposition of an aligned neutron pair and an aligned proton pair rather than independent neutron and proton alignments. This can affect the experimental signature of the alignment. In particular, in



47Ti

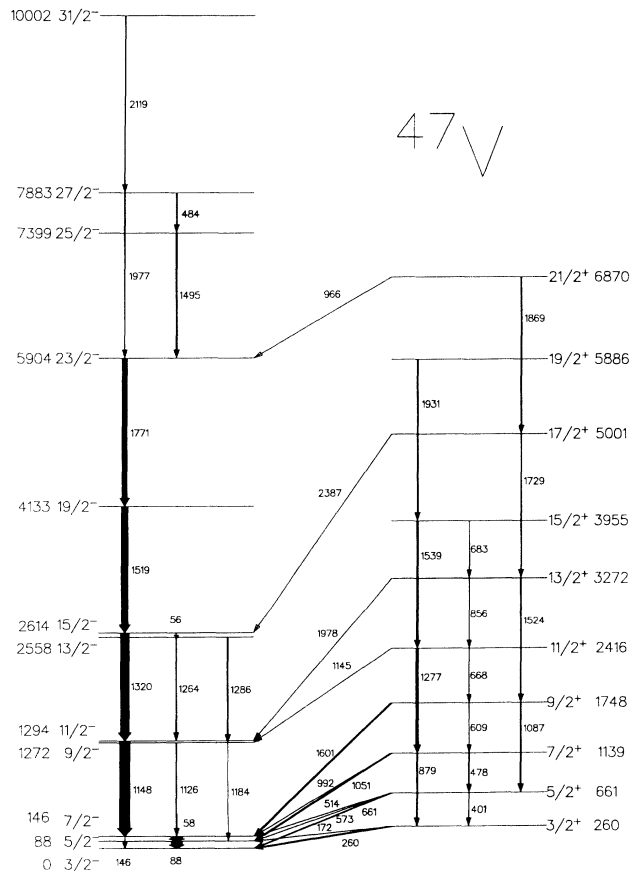
FIG. 3. Level scheme of ^{47}Ti . Level and transition energies are in keV, quoted to the nearest keV.

TABLE V. States and transitions in ^{48}Cr .

E_i (keV)	E_f (keV)	E_γ (keV)	Int. % ^a	A^b	J_i^π	J_f^π
752	0	752	100	1.21(7)	2^+	0^+
1858	752	1106	97	1.3(1)	4^+	2^+
3444	1858	1586	97	1.4(1)	6^+	4^+
3531	1858	1673	6		(5^-)	4^+
	3444	87	0.6			6^+
4062	3531	531	5		(6^-)	(5^-)
4512	3444	1068	5		(7^+)	6^+
5318	3444	1874	80	1.4(2)	8^+	6^+
	4512	806	2			(7^+)
7062	5318	1744	65	1.4(2)	10^+	8^+
8408	7062	1347	42	1.6(3)	12^+	10^+
10430	8408	2022	11		(13^+)	12^+
10609	8408	2201	13		(14^+)	12^+

^aNormalized to 100 for the 752-keV decay.

^bSee text, Sec. II. Uncertainties are 1σ .



47V

FIG. 4. Level scheme of ^{47}V . Details as in Fig. 3.

the absence of neutron-proton pairing and assuming identical neutron and proton single-particle levels, neutrons and protons will align simultaneously in an $N = Z$ nucleus. In the case of the $f_{7/2}$ shell, this would imply a total alignment of $12\hbar$. In contrast, the inclusion of the residual n - p interaction results in the two aligned two-quasiparticle states being split, with the result that the alignment can occur in two steps of $6\hbar$, separated in rotational frequency.

The result of Fig. 8 is thus clearly consistent with the prediction of Ref. [12], in that the data show a distinct first alignment step of only $6\hbar$. It would clearly be of considerable interest to search for the predicted second alignment. Alternatively, the presence of n - p correlations could be tested by a study of the g factors of the states in the region of the alignment.

The positive-parity bands in ^{47}V and ^{47}Cr , as well as the 1^- and 4^- bands of ^{48}Cr , have almost the same moments of inertia as that of ^{48}Cr , near $10\hbar^2\text{MeV}^{-1}$. This suggests that in each case the $d_{3/2}$ hole acts only as a spectator. There is speculation that ^{48}Cr may become super- or hyperdeformed at higher energy [5]. No evidence for this was found in this work.

B. Mirror symmetry, ^{47}Cr - ^{47}V and ^{49}Mn - ^{49}Cr

The mirror symmetry of the two $T = \frac{1}{2}$ systems near ^{48}Cr is remarkably good. Not only are the level schemes of ^{47}V and ^{47}Cr closely similar, as are those of ^{49}Cr and ^{49}Mn [6], but so also are the decay branchings from corresponding levels, as may be seen by comparing the spectra or from Tables II and III. The rotational nature of the yrast band of ^{47}V is seen most clearly in the $\hbar\omega$ vs J diagram, Fig. 9, from which an average moment of inertia $\mathcal{I} = 12\hbar^2\text{MeV}^{-1}$ is found.

The Coulomb energy difference $\Delta E_C = E_x(^{47}\text{Cr}) - E_x(^{47}\text{V})$ relative to that for the ground state was presented and discussed at length in Ref. [13]. Figure 10, from that work, shows the comparison of ΔE_C values for

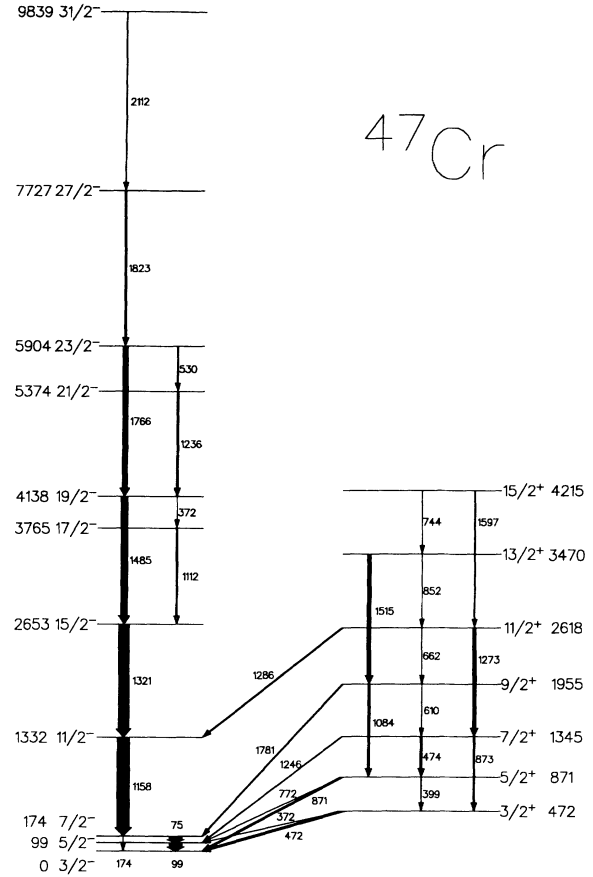


FIG. 5. Level scheme of ^{47}Cr . Details as in Fig. 3.

the $A = 47$ and 49 systems. The interpretation given in Refs. [13,14] is that the sudden shift near $J = \frac{17}{2}$ results from a decrease in overlap of nucleons in the even group brought about by a rotation-driven spin alignment. It also seems likely that the smaller variation in ΔE_C at lower spin results from the more gradual alignment of

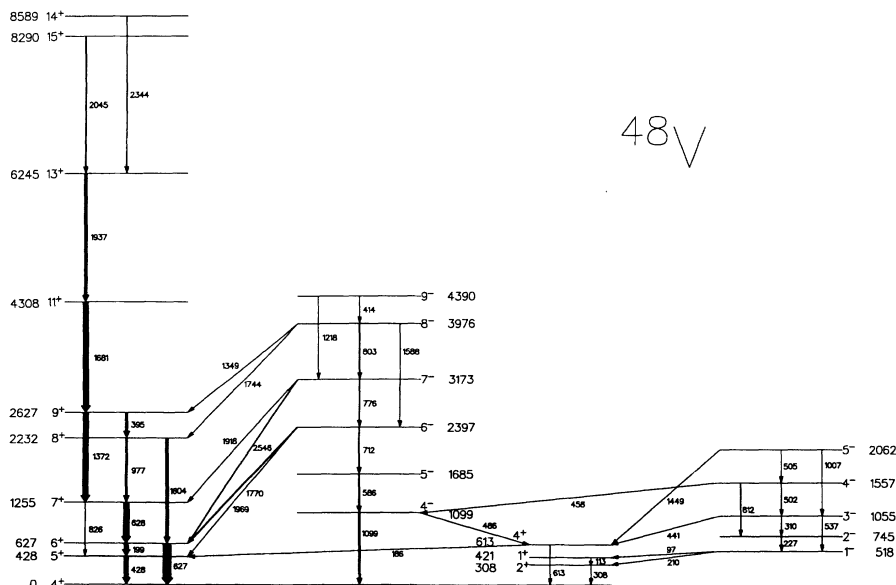


FIG. 6. Level scheme of ^{48}V . Details as in Fig. 3.

the three-nucleon group. While the latter behavior is consistent with a shell-model description, the former is not, and seems only to be accounted for by a rotational alignment.

C. Cross-conjugate symmetry, ^{47}V - ^{49}Cr and ^{47}Ti - ^{49}V

Within the context of a single shell, level spectra and, with some phase changes, wave functions of cross-conjugate nuclei are identical. Such a cross-conjugate pair exists in ^{47}V and ^{49}Cr , and, of course, their mirror nuclei ^{47}Cr and ^{49}Mn . The yrast levels of the first pair are compared in Figs. 11(a) and 11(b). While there is a general similarity of level behavior in the form of rotational spacing, with signature doublets, there are significant differences, particularly at low spin and near $J = \frac{19}{2}$. The

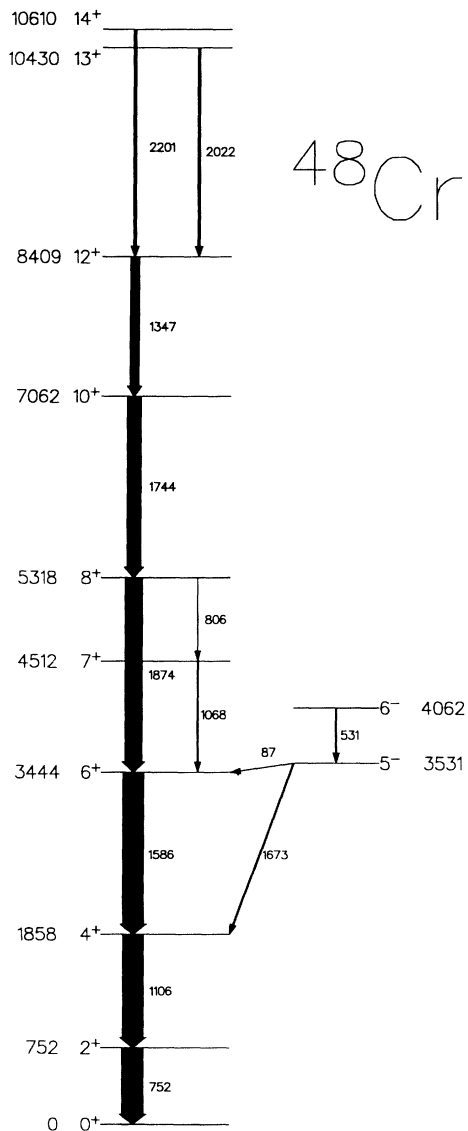


FIG. 7. Level scheme of ^{48}Cr . Details as in Fig. 3.

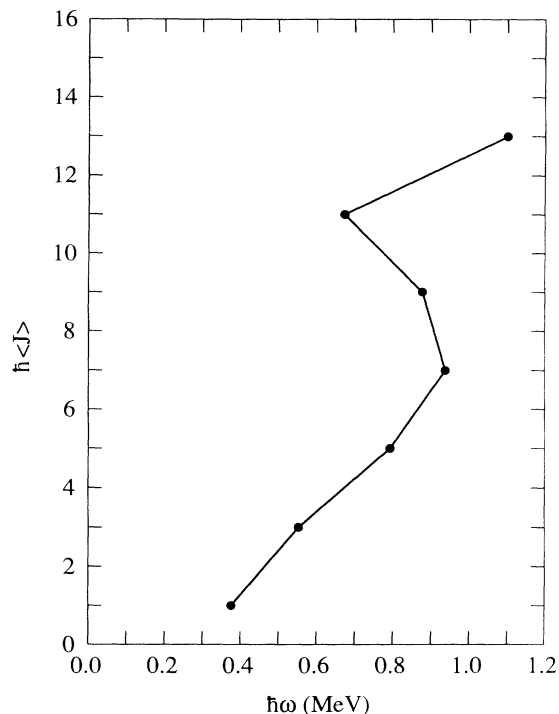


FIG. 8. Spin plotted against rotational energy $\hbar\omega$ for the positive-parity states in ^{48}Cr .

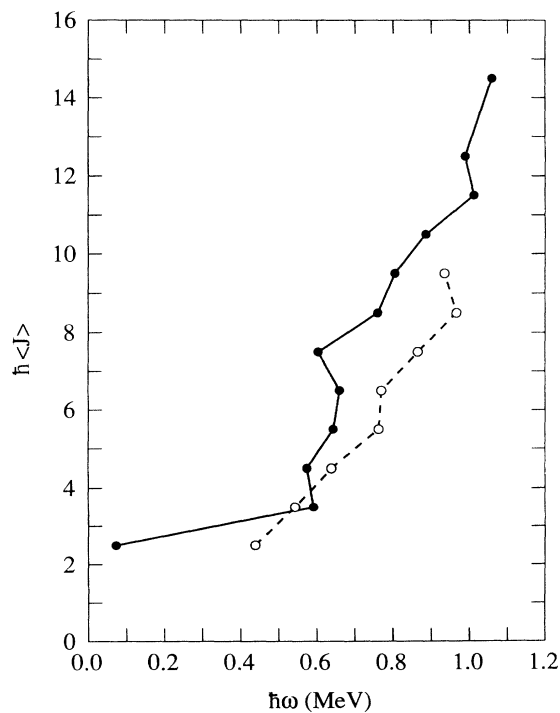


FIG. 9. Spin plotted against rotational energy for ^{47}V . Solid circles, negative-parity states; open circles, positive-parity states.

low-spin failure of symmetry may be traceable to the intrusion of either the $p_{3/2}$ or the sd shell, through single or double particle-hole excitations. We have no explanation of that at higher spin, unless it is related to the rotational level crossing made evident in the Coulomb energy differences and in ^{48}Cr . A second possibility is that the $\frac{23}{2}^-$ level in ^{47}V is, in fact, a second $\frac{19}{2}^-$, with the $J \rightarrow J$ dipole transition mistaken for a stretched $E2$. However, searches for other transitions made possible in that case were unsuccessful, both in ^{47}V and in ^{47}Cr . Another cross-conjugate pair is ^{47}Ti - ^{49}V , whose negative-parity states are shown in Figs. 11(c) and 11(d). The levels for ^{49}V are taken from Ref. [7]. The most obvious deviations from symmetry in the level schemes occur between spin $\frac{17}{2}^-$ and the $(f_{7/2})^{2+3}$ band termination at $\frac{27}{2}^-$.

V. SUMMARY

The use of isotopically tagged γ spectroscopy has allowed significant extensions to the level schemes of the five $f_{7/2}$ shell nuclei ^{47}Ti , $^{47,48}\text{V}$, $^{47,48}\text{Cr}$. With ^{49}Cr and ^{49}Mn [6], ^{47}V and $^{47,48}\text{Cr}$ make up a small region of deformation in the center of the shell, showing many of the features of more familiar regions of permanent deformation. At the same time, shell-model characteristics, such as cross-conjugate symmetry and band termination, are still apparent.

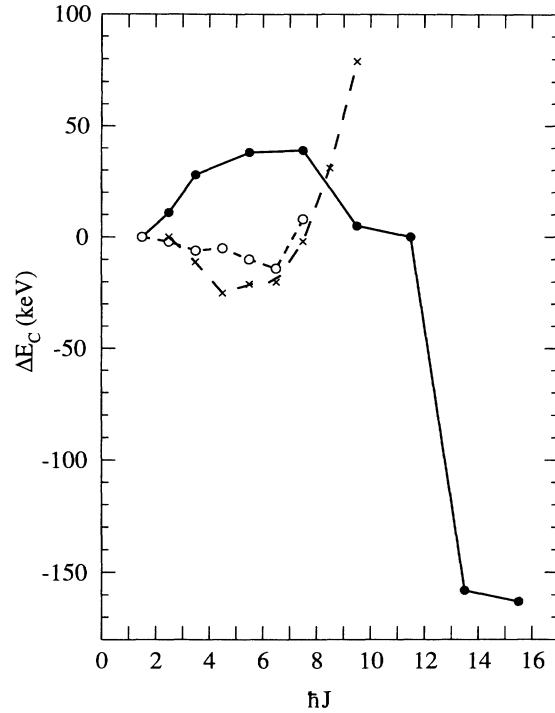


FIG. 10. Dependence of the Coulomb displacement energy ΔE_C on spin for the negative-parity levels of the mirror nuclei at $A = 47$ (solid circles) and $A = 49$ (crosses), and for the positive-parity levels of $A = 47$ (open circles).

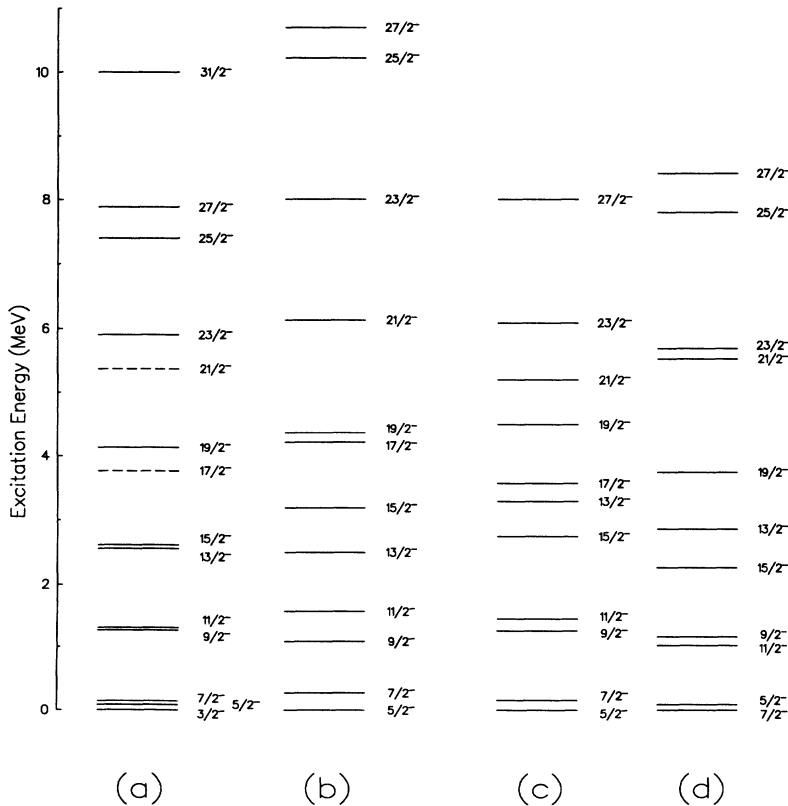


FIG. 11. Comparison of the negative-parity levels of the cross-conjugate nuclei (a) ^{47}V (dashed levels are from the mirror nucleus ^{47}Cr) and (b) ^{49}Cr ; (c) ^{47}Ti and (d) ^{49}V .

ACKNOWLEDGMENTS

This work was supported by the U.K. Science and Engineering Research Council and by the National Science and Engineering Research Council of Canada.

-
- [1] W. Kutschera, B. A. Brown, and K. Ogawa, *Riv. Nuovo Cimento* **1**, 12 (1978).
 - [2] D. E. Alberger, *Nucl. Data Sheets* **45**, 557 (1985).
 - [3] T. W. Burrows, *Nucl. Data Sheets* **48**, 1 (1986).
 - [4] T. W. Burrows, *Nucl. Data Sheets* **48**, 569 (1986).
 - [5] I. Ragnarsson, private communication.
 - [6] J. A. Cameron, M. A. Bentley, A. M. Bruce, R. A. Cunningham, W. Gelletly, H. G. Price, J. Simpson, D. D. Warner, and A. N. James, *Phys. Lett. B* **235**, 239 (1990).
 - [7] J. A. Cameron, M. A. Bentley, A. M. Bruce, R. A. Cunningham, W. Gelletly, H. G. Price, J. Simpson, D. D. Warner, and A. N. James, *Phys. Rev. C* **44**, 1882 (1991).
 - [8] A. N. James, T. P. Morrison, K. Y. Ying, K. A. Connell, H. G. Price, and J. Simpson, *Nucl. Instrum. Methods A* **267**, 144 (1988).
 - [9] J. Simpson, M. Bates, C. Brookes, and P. J. Nolan, *Nucl. Instrum. Methods A* **269**, 209 (1988).
 - [10] J. A. Cameron, D. G. Popescu, and J. C. Waddington, *Phys. Rev. C* **44**, 2358 (1991).
 - [11] A. L. Goodman, *Adv. Nucl. Phys.* **11**, 263 (1979).
 - [12] J. A. Sheikh, N. Rowley, M. A. Nagarajan, and H. G. Price, *Phys. Rev. Lett.* **64**, 376 (1990).
 - [13] J. A. Cameron, M. A. Bentley, A. M. Bruce, R. A. Cunningham, W. G. Price, J. Simpson, D. D. Warner, A. N. James, W. Gelletly, and P. Van Isacker, *Phys. Lett. B* **319**, 58 (1993).
 - [14] J. A. Sheikh, P. Van Isacker, D. D. Warner, and J. A. Cameron, *Phys. Lett. B* **252**, 314 (1990).